Optimization of Passive and Active Electromechanical Suspension Systems

Willian Minnemann Kuhnert, Marcos Silveira, Paulo J. Paupitz Gonçalves

Faculty of Engineering of Bauru - UNESP. Av. Eng. Luiz Edmundo C. Coube 14-01, Vargem Limpa, 17033-360 - Bauru - SP, Brazil. willian.kuhnert@feb.unesp.br, m.silveira@feb.unesp.br, paulo.jpg@feb.unesp.br

Abstract: The study of regenerating systems to make use of wasted energy has become an important subject in the development of new mechanical systems. In the case of automobile suspension systems, one way that it is possible to harvest energy is by coupling an electrical system to the mechanical system, and use the harvested energy to active control. The automobile suspension systems are necessary primarily to improve handling stability and passenger comfort, though they are usually competing objectives, where improving one degrades the other. The aim of this paper is to study a simplified suspension model, composed by a single degree of freedom (SDOF) mechanical system (mass, spring and damper) and a coupled SDOF electrical circuit (inductor, resistor and capacitor) that converts mechanical into electrical energy, in order to improve both comfort to passengers and handling, by using the restored energy for active control. As these are competing objectives, a multi-objective optimization procedure with Genetic Algorithm is used. Feedforward strategy is employed to reduce vibration and increase electrical energy harvested. At first, from the mathematical model obtained by Lagrangian approach, a frequency response analysis is derived by considering harmonic excitation or the Impedance Method. The displacement transfer function, also known as displacement transmissibility, and the charge transfer function are obtained and analyzed, i.e., the equations defining the resonance frequencies (poles) and the anti-resonance frequency (zero) are defined. Second, passive control with multi-objective optimization is carried out by using Genetic Algorithm with the objective of minimization of the area under the transmissibility response as a function of the frequency and the maximization of the charge. This is done by adjusting the dissipation coefficients (damping coefficient and resistance) to a constrained problem. Finally, active control is carried out using feedforward strategy. The results obtained are compared to the same model without active control in order to decide which one is better for the purposed problem. It is shown that it is very possible to develop an optimized electromechanical suspension system for automobiles which conciliates the energy harvested and the displacement transmissibility, resulting in improved handling and comfort for passengers.

Keywords: Electromechanical suspension, Multi-Objective Optimization, Displacement transmissibility, Energy harvesting

INTRODUCTION

The study of regenerating systems to make use of wasted energy has become an important subject in the development of new mechanical systems. This is the case of automobile suspension systems which have two main important objectives: handling stability and comfort. These are usually competing objectives, where improving one degrades the other.

In a typical vehicular damping system, viscous dampers dissipate energy as heat, i.e., energy is lost to the environment. The implementation of an energy recovery system allows part of this energy to be reused. Therefore, automotive and rail suspension systems are among the various application possibilities of electromechanical devices. These devices have advantages compared to conventional viscous damper, such as ease of application of an active control and parameter setting, broader band of vibration attenuation, and the possibility of system energy recovery (Amati *et al.* 2011, Tonoli *et al.* 2013). The electromagnetic system may also be used in a semi-active suspension, with the control being realized by the electrical components of the device, facilitating its implementation.

Some experimental electromagnetic suspension systems have been built. Systems using rotary motors and linear to angular motion conversion showed good relationship of recovered energy and weight (Amati *et al.* 2011, Tonoli *et al.* 2013). This type of configuration considerably reduces the total weight compared to other systems already developed. Its final weight was only about 20 % higher than a hydraulic suspension system, which can be considered a relatively low weight. This shows that the development of this type of suspension system has advanced significantly towards the viability of its application.

An electromagnetic system consisting of a DC motor and a ball-screw mechanism was demonstrated by Kawamoto et al. (2007). The linear vibration motion is converted into torque input signal to the DC motor. The electromagnetic shock absorber uses magnetic force as damping, and this force can be electrically controlled by regulating the induced current. The use of active control in the suspension system proved that a considerable reduction of vibrations is possible with a

positive energy balance.

At Zuo *et al*. (2010) and Zuo and Zhang (2013), the authors developed a damper which can harvest energy and demonstrated the balance between the amount of energy recovered from the system and passenger comfort. Available energy in the system varies between 100 W and 400 W in midsize cars running in good and medium condition roads, and depends on vehicle speed, road roughness and tire stiffness. Therefore, the compromise between recovered energy, passenger comfort and stability of the vehicle depends on the type of road on which the vehicle travels, and a control algorithms must be developed to optimize the dynamic behavior in every situation (Ebrahimi *et al*. (2010)).

The conventional elements used in suspension systems are usually springs and dampers. In some cases, the spring and damper elements are developed in a way that results in nonlinear behavior. In other situations, the springs and dampers can be modeled as linear elements, but the kinematics of the suspension system results in geometric nonlinear behavior. Pontes *et al*. (2014) explored the dynamical behavior of an electromagnetic suspension system with nonlinear stiffness. It was observed that the electrical parameters are highly responsible for the behaviour of the resulting mechanical damping effect, and indicates that the capacitance can be used as a control parameter.

The aim of this work is to study a simplified suspension model which takes into account a secondary electrical circuit that converts mechanical into electrical energy, thus acting as a damper. The vertical dynamics of a SDOF mechanical system with coupled electrical system is analyzed, with a view to improve comfort to passengers and to improve handling. As these are competing objectives, a multi-objective optimization procedure with genetic algorithm is used. Feedforward control strategy is employed to reduce vibration and increase electrical energy harvested.

PROBLEM FORMULATION

The system considered in this paper is depicted in Fig. 1 which represents a mass supported by mechanical components (spring and damper) and coupled electrical circuit including a resistor, an inductor and a capacitor. This system is subjected to harmonic base excitation. The quarter-car model, as this system is also known, is used in order to investigate the suspension system performance concerning the charge collected and the comfort provided, instead of the whole vehicle's dynamic behavior.
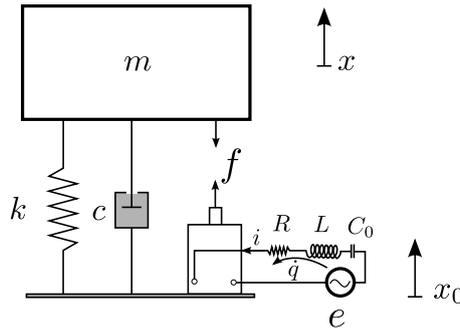

Figure 1 – Electromechanical suspension system subjected to base excitation.

The equations of motion of this system can be achieved by Lagrangian approach for the mechanical and eletrical subsystems, as described in the literature by Crandall (1968) and by Preumont (2006). The set of two differential equations can be written as

$$m\ddot{x} + c\dot{x} + kx - T\dot{q} = c\dot{x}_0 + kx_0 \tag{1}$$

$$L\ddot{q} + R\dot{q} + \frac{q}{C_0} + T\dot{x} = T\dot{x}_0 + e \tag{2}$$

where the mechanical system parameters m, k, and c are, respectively, the mass, stiffness and damping coefficients. The electrical system parameters L, R and C_0 are, respectively, the inductance, resistance and capacitance coefficients, and e is the external electric tension. The term T which couples the two equations is defined as the *Transducer Constant* (equal to the product of the length of the coil exposed and the magnetic flux). This term can have SI unit Volt×second/meter or Newton/Ampere. The dependent variables are the displacement of the mass (x) and the charge (q), while x_0 is the base displacement amplitude.

Frequency Response Analysis

Considering harmonic motion of the system described by equations 1 and 2 in the form of complex exponentials, such that $x(t) = Xe^{j\omega t}$, $x_0(t) = X_0 e^{j\omega t}$, $q(t) = Qe^{j\omega t}$ and $e(t) = Ee^{j\omega t}$, the equations of motion are written in the frequency domain as

$$(-\omega^2 m + j\omega c + k)X - j\omega T Q = (j\omega c + k)X_0 \tag{3}$$

$$\left(-\omega^2 L + j\omega R + \frac{1}{C_0}\right)Q + j\omega TX = j\omega TX_0 + E \tag{4}$$

A procedure to obtain the transmissibility frequency response consists of eliminating the charge amplitude Q.

The motion of electromechanical system is better described in terms of impedance, since it allows the modeling and analysis of numerical models that can be easily measured by experimental tests. The mechanical impedance is the ratio of a sinusoidal input force to the resulting velocity. The ratio relating the force and the resulting displacement is known as dynamic stiffness.

Defining the following impedance terms

$$Z_m = -\omega^2 + j\omega c + k \tag{5}$$

$$Z_e = -\omega^2 L + j\omega R + \frac{1}{C_0} \tag{6}$$

$$Z_s = j\omega c + k \tag{7}$$

$$X = \left(Z_e Z_m - \omega^2 T^2\right)^{-1}\left(\left(Z_e Z_s - \omega^2 T^2\right)X_0 + j\omega TE\right) \tag{8}$$

By removing the coupling term T, the system becomes a spring-mass-damper system. The terms of the denominator are defined by two terms $Z = Z_m - \frac{\omega^2 T^2}{Z_e}$ which can be seen as the Mechanical and Electrical Impedance (dynamic stiffness), respectively. Both mechanical, electrical and the total impedance are plotted in the complex plane of Fig. 2, illustrating the influence of the electrical sub-system into the mechanical sub-system. The blue line represents the mechanical impedance for different values of excitation frequency and the green line represents the impedance composed by the coupling system and the electrical sub-system. The total impedance Z is represented by the red line. For low and high frequencies the total impedance tends to approach the mechanical impedance.
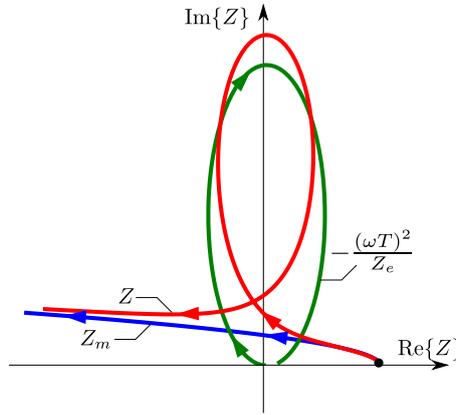

Figure 2 – Real and Imaginary parts of the mechanical, electrical and total impedance

For the case of the electrical charge Q, it is also possible to obtain the transfer function relating the base motion with the electrical charge by eliminating the displacement variable X such that

$$Q = \left(Z_m Z_e - \omega^2 T^2\right)^{-1}\left(j\omega T\left(Z_m - Z_s\right)X_0 + Z_m E\right) \tag{9}$$

The transfer functions (X/X_0 and Q/X_0) for base excitation are shown in Fig. 3. The displacement transfer function (X/X_0) indicates the gain the sprung mass has when it is harmonically excited in its base under each excitation frequency. The charge transfer function (Q/X_0) indicates how much energy is obtained in the electrical sub-system when the mass is excited as aforementioned.

Neglecting the variables relate to the energy dissipation (c viscous damping and R electrical resistance) it is possible to obtain the equations defining the resonance frequencies (Poles), defined as

$$\omega_1^2 = \frac{\omega_m^2 + \omega_e^2 + \alpha\tau^2 - \sqrt{(\omega_m^2 - \omega_e^2)^2 + \alpha\tau^2(\alpha\tau^2 + 2(\omega_m^2 + \omega_e^2))}}{2} \tag{10}$$

$$\omega_2^2 = \frac{\omega_m^2 + \omega_e^2 + \alpha\tau^2 + \sqrt{(\omega_m^2 - \omega_e^2)^2 + \alpha\tau^2(\alpha\tau^2 + 2(\omega_m^2 + \omega_e^2))}}{2} \tag{11}$$

where $\omega_m = \sqrt{k/m}$, $\omega_e = \sqrt{1/LC_0}$ are the natural frequencies of the uncoupled mechanical and electrical systems, $\tau = T/m$ and $\alpha = m/L$. The systems also presents a anti-resonance frequency (zero) defined as

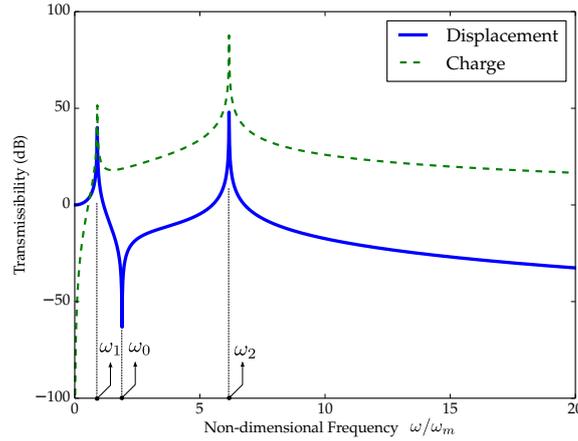$$\omega_0 = \frac{\omega_e \omega_m}{\sqrt{\omega_m^2 + \alpha\tau^2}} \tag{12}$$

Figure 3 – Transmissibility as a function of the excitation frequency (a small amount of damping was considered to plot this figure)

PASSIVE CONTROL

In this section optimization of the system response is performed using different strategies. The optimization is performed using Genetic Algorithm based on the work of Deb *et al*. (2002) using the implementation in C-language of this algorithm. The objective is to minimize the area under the transmissibility response as a function of the frequency and to maximize the the area under the transfer function with Charge as output and base displacement as input. This is done by adjusting the dissipation coefficients c and R, according the the following constrained problem.

$$\underset{c,R}{\text{minimize}} \quad J_1, J_2$$

$$\text{subjected to} \quad 1 \le c \le 2000$$

$$1 \le R \le 200$$

where, the objective functions J_1 and J_2 are defined as

$$J_1 = \frac{1}{n}\sum_{i=1}^{n}\left|\frac{X(\omega_i)}{X_0(\omega_i)}\right| \tag{13}$$

$$J_2 = \frac{1}{\frac{1}{n}\sum_{i=1}^{n}\left|\frac{Q(\omega_i)}{X_0(\omega_i)}\right|} \tag{14}$$

The parameters used in the analysis where set according to Pontes Jr *et al* (2015) and are shown in Table 1

Table 1 – Values used in the Optimization

Parameter	Value
Mass [m]	250 [kg]
Stiffness [k]	40000 [N/m]
Viscous Damping [c]	Variable [N/m]
Inductance [L]	0.76 [H]
Resistance [R]	Variable [Ohms]
Capacitance [C_0]	0.0014[Farad]
Electromechanical Coupling [T]	500 [N/Amp]

The parameters used in the optimization procedure are shown in Table , with

After performing the optimization, the Pareto Front was plotted in fig. 4(a). As expected, the Pareto front shows a inverse relationship between the displacement amplitude and the charge flowing in the electrical circuit.

Finally, for different values of mass, it was possible to obtain different Pareto Fronts, shown in fig. 4(b). It can be seen that the influence of the mass on the system only shifts the Pareto front, without changing its shape very much.

For the points (1), (2) and (3) presented in fig. 4(a), it was possible to obtain the transfer functions (X/X_0 and Q/X_0) behaviors, shown in fig. 5. The point (1) correspond to a situation where the reduction of displacement is a minimum, and it produces the maximum charge for this condition. The point (2) corresponds to a situation where the Charge is a maximum. It is clear that the displacement is also very large at the resonance frequencies. The point (3) corresponds to a trade-off relationship to have relative low displacement at the resonance, but still have some electrical charge in the electrical circuit.

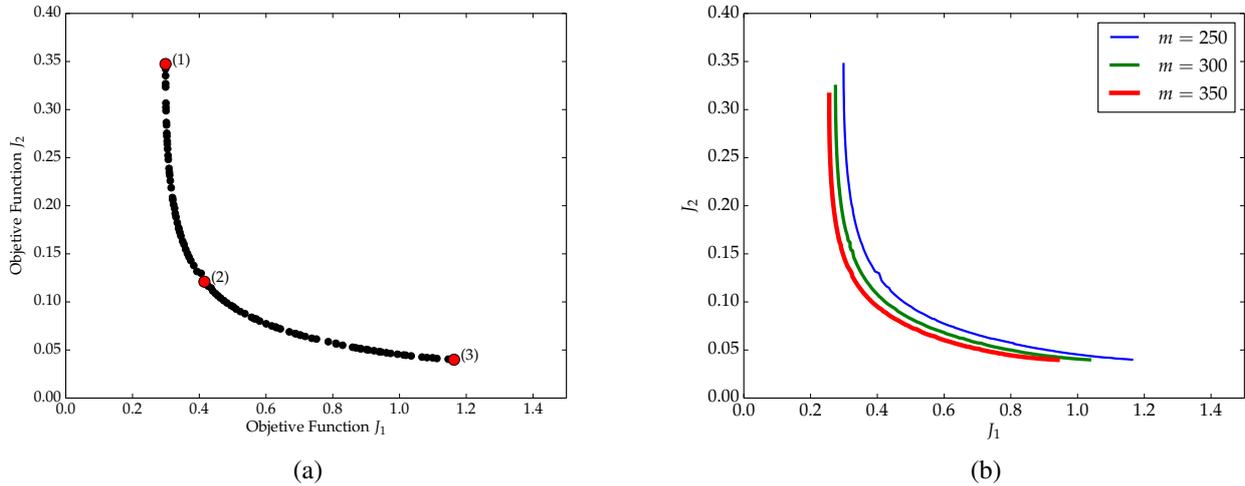| Parameter	Value
Population Size	100
Number of Generations	80
Probability of crossover	0.9
Probability of mutation	0.5
Distribution index for crossover	10
Distribution index for mutation	20

(a)

(b)

Figure 4 – Pareto Front. (a) obtained for values of viscous damping c and electrical resistance R and (b) influence of values of the system mass m

ACTIVE CONTROL

In this section the strategy of feedforward control is considered as a solution to reduce the vibration of the system. Feedforward control was extensively studied in many applications and its principles are discussed in the book by Fuller (1996) and also in references such as Brennan and McGowan (1997) and Snyder and Tanaka (1993).

The diagrams shown in Fig. 6 illustrate the idea of active control considered in this paper. The feedforward control makes use of a sensor to measure the disturbance input, which is in this case the displacement of the base. This signal feeds a controller which converts the disturbance to a control input. In this case, it converts to electrical voltage.

In simple terms, the idea of feedforward control is to provide a secondary input (*control input*) that cancels out (or minimizes) the effect of the disturbance. The control input is linear related to the disturbance input.

Consider the block diagram shown in Fig. 6(b), where the block H_{ff} describes the feedforward control filter, and the blocks H_d and H_c describe the transfer functions relating the contributions of the disturbance X_0 to the response X and the contributions of the applied voltage E to the response X, respectively.

If the interest is to control the displacement of the mass, it is necessary to consider the expression relating X, X_0 and
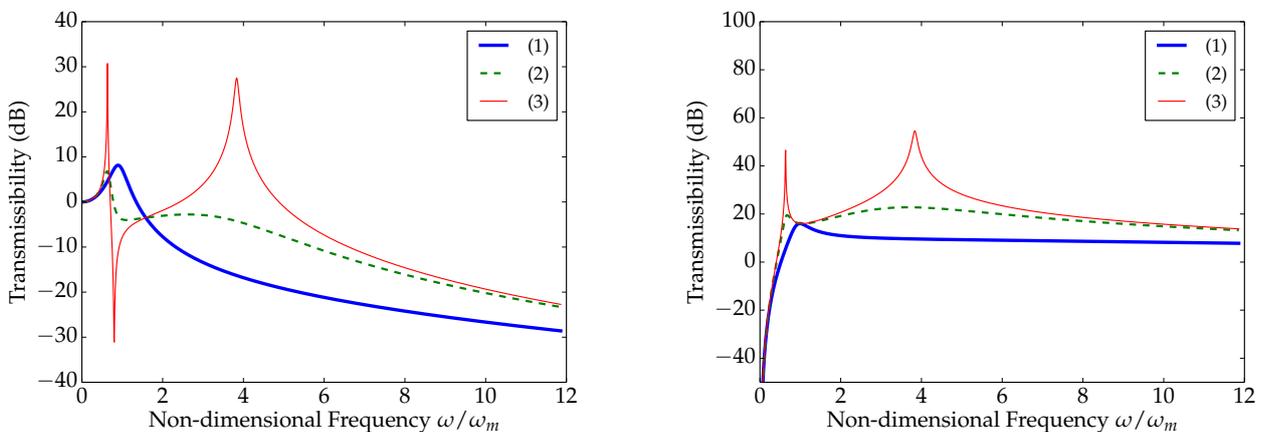

Figure 5 – Frequency response for three values extracted from the Fig. 4. (a) Displacement (transmissibility) and (b) Charge (Transmissibility). (1) $c = 3.92$ and $R = 177.48$, (2) $c = 1.03$ and $R = 38.99$, (3) $c = 1.00$ and $R = 1.00$
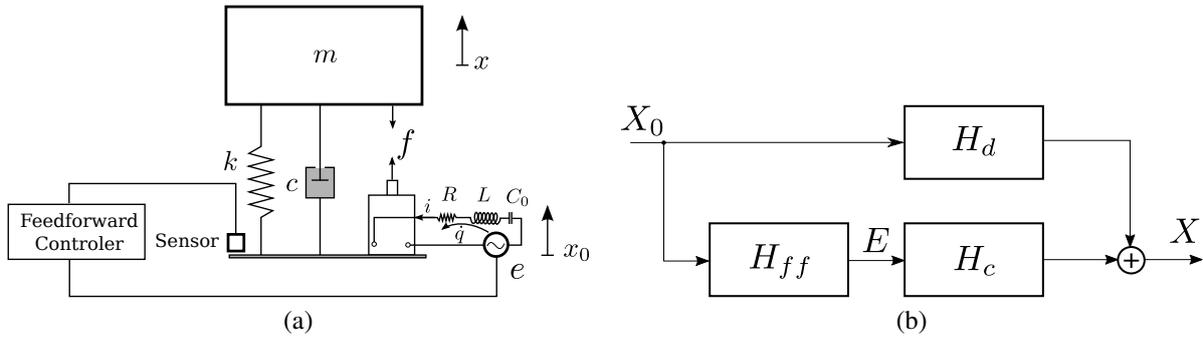
Figure 6 – The feedforward strategies for active control. (a) schematic idea of feedforward controle and (b) block diagram

E:

$$X = \left(Z_e Z_m - \omega^2 T^2\right)^{-1} \left(\left(Z_e Z_s - \omega^2 T^2\right) X_0 + j\omega T E\right) \tag{15}$$

The transfer function H_d is obtained by making $E = 0$ and H_c is obtained by making $X_0 = 0$ in equation 15. The total response X can be written as

$$X = H_d X_0 + H_c E = \left(H_d + H_c H_{ff}\right) X_0 \tag{16}$$

In this case, it is possible to find the optimal feedforward control by making $X = 0$, which gives the following

$$E_{opt} = j\left(\frac{Z_e}{\omega T}\left(j\omega c + k\right) - \omega T\right) X_0 \tag{17}$$

If this value of voltage is applied to the equation 6, the displacement of the mass is canceled. This occurs because the impedance match between the mechanical and electrical inputs.

However, the control effort in terms of the total disturbance X_0, shown in Fig. 7(a), is very high at low frequencies, which can make the controller implementation impracticable. The phase relative to the disturbance X_0 is shown in Fig. 7(b)
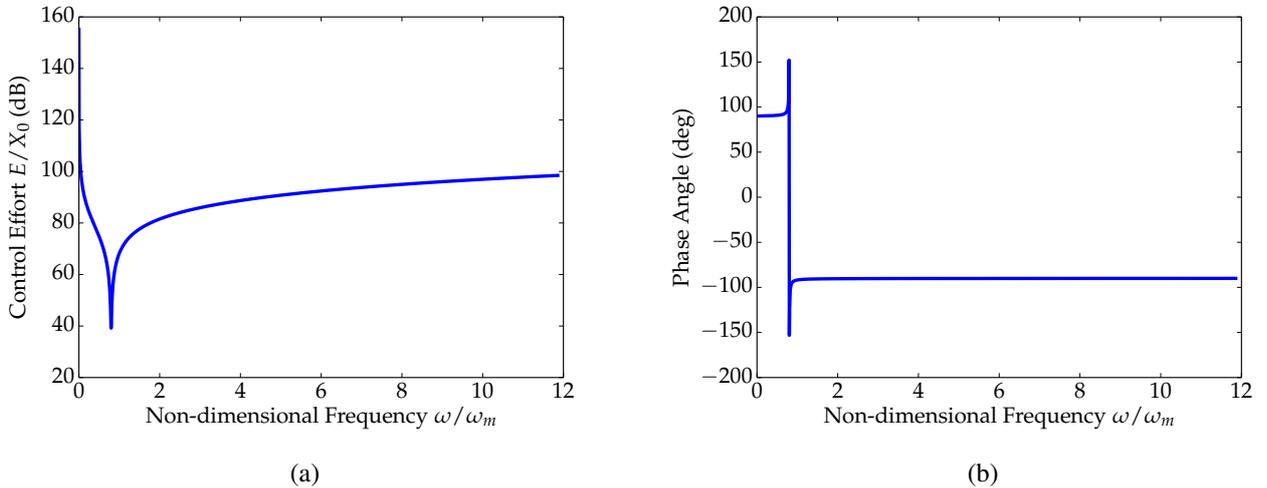

Figure 7 – Optimal feeforward control. (a) control effort and (b) phase angle

If the magnitude of the optimal control E_{opt} in eq. 17 is expanded, there is a term defined by $\frac{k^2}{\omega^2 C_0^2 T^2}$ which has a frequency dependence in the denominator. This term is responsible for large values of control voltage in the low frequency range of Fig. 7. There are some possibilities of reducing the control effort in the low frequency region. To do this, it is necessary to change the term $\frac{k^2}{\omega^2 C_0^2 T^2}$.

Two possible changes in the controller were investigated and the magnitude of the control voltage is shown in Fig. 8. The first solution is to eliminate the term k from equation 17, consequently removing the aforementioned term from the controller effort, which produces a control voltage E_1. In the second case E_2, the term is changed to $\frac{k^2}{\omega_a^2 C_0^2 T^2}$, where

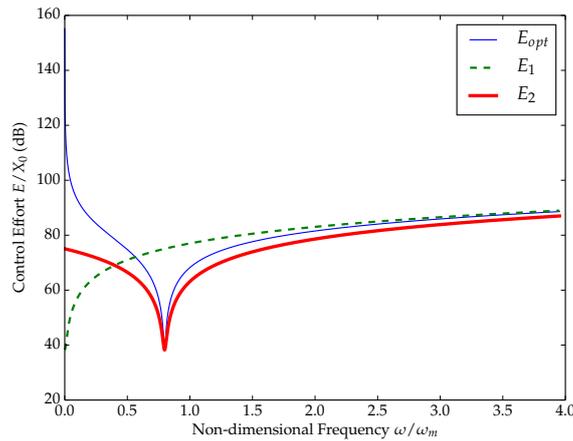$$\omega_a = \sqrt{\frac{k}{C0\left(T^2 + kL\right)}}.$$

Figure 8 – The control effort for optimal feedforward control

By changing the feedforward optimal controller, there is a reduction in the performance of the controller. The performances are shown in the results of Fig. 9(a) (and in the detail for the first resonance frequency Fig. 9(b)). The performance without control is the third situation shown in Fig. 5, while the performances E_1 and E_2 are both from the aforementioned adapted optimal controllers.
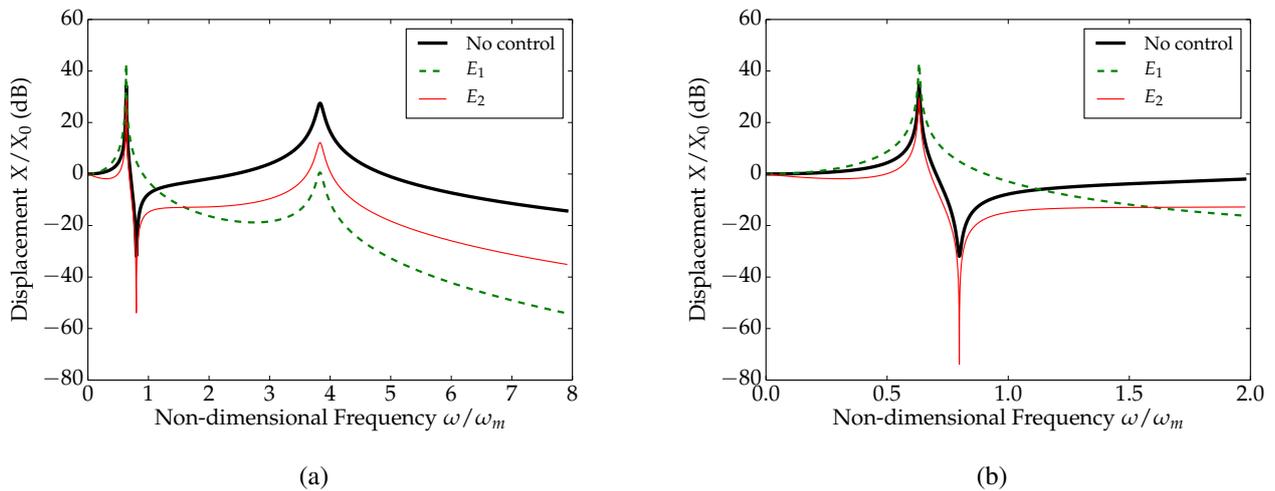

(a)

(b)

Figure 9 – Comparison of the transmissibility for the system without control and with modified feedforward control (a). The detail of the first resonance (b).

CONCLUSION

By observing Fig. 9, control E_1 is the best choice applied for the system at higher excitation frequencies, while control E_2 is the best choice applied for the system at lower frequencies. Moreover, it can be observed from Fig. 8 that control E_1 requires less power at lower frequencies and more power at higher frequencies when compared to control E_2. The system without active control has the worst behaviour when compared to the others, but it can collect and store energy instead of using it. The systems with active control can use the collected energy to reduce the displacement transmissibility, resulting in improved comfort for passengers.

ACKNOWLEDGMENTS

REFERENCES

Amati, N., Festini, A. and Tonoli, A., 2011, "Design of electromagnetic shock absorbers for automotive suspensions", Vehicle System Dynamics, Vol.49, No.12, 1913-1928.

Brennan, M. C. and McGowan, A. M. R., 1997, "Piezoelectric power requirements for active vibration control". Proceedings of the 4th Smart Structures and Materials, pp. 660-669.

Crandall, S. H., 1968, "Dynamics of mechanical and electromechanical systems", McGraw-Hill.

Deb, K., Pratap, A., Agarwal, S. and Meyarivan, T. A. M. T., 2002, "A fast and elitist multiobjective genetic algorithm: NSGA-II", IEEE transactions on evolutionary computation, Vol.6, No.2, 182-197.

Ebrahimi, B., Bolandhemmat, H., Khamesee, M. B. and Golnaraghi, F., 2011, "A hybrid electromagnetic shock absorber for active vehicle suspension systems", Vehicle System Dynamics, Vol.49, No.1-2, 311-332.

Fuller, C. C., Elliott, S. and Nelson, P. A., 1996, "Active control of vibration", Academic Press.

Kawamoto, Y., Suda, Y., Inoue, H. and Kondo, T., 2007, "Modeling of electromagnetic damper for automobile suspension", Journal of System Design and Dynamics, Vol.1, No.3, 524-535.

Pontes Jr, B. R., Silveira, M., Mazotti, A. C., Gonçalves, P. J. and Balthazar, J. M., 2015, "Contribution of electrical parameters on the dynamical behaviour of a nonlinear electromagnetic damper", Nonlinear Dynamics, Vol.79, No.3, 1957-1969.

Preumont, A., 2006, "Mechatronics: dynamics of electromechanical and piezoelectric systems", Vol. 136, Springer Science & Business Media.

Snyder, S. D. and Tanaka, N., 1993, "On feedforward active control of sound and vibration using vibration error signals", The Journal of the Acoustical Society of America, Vol.94, No.4, 2181-2193.

Tonoli, A., Amati, N., Detoni, J. G., Galluzzi, R. and Gasparin, E., 2013, "Modelling and validation of electromechanical shock absorbers", Vehicle System Dynamics, Vol.51, No.8, 1186-1199.

Zuo, L., Scully, B., Shestani, J. and Zhou, Y., 2010, "Design and characterization of an electromagnetic energy harvester for vehicle suspensions", Smart Materials and Structures, Vol. 19, No. 4, 045003.

Zuo, L. and Zhang, P. S., 2013, "Energy harvesting, ride comfort, and road handling of regenerative vehicle suspensions", Journal of Vibration and Acoustics, Vol.135, No.1, 011002.

RESPONSIBILITY NOTICE

The authors are the only responsible for the material included in this paper.